ORIENTATION OF MOMS-02/D2 AND MOMS-2P IMAGERY

H. Ebner, T. Ohlhof, E. Putz

Chair for Photogrammetry and Remote Sensing
Technical University Munich, D-80290 Munich, Germany
Phone: +49-89-2892 2671, Fax: +49-89-280 95 73
E-Mail: timm@photo.verm.tu-muenchen.de

Commision III, Working Group 1

KEY WORDS: Orientation, Three-Line, CCD, Bundle Block Adjustment, MOMS

ABSTRACT

This paper deals with the orientation of 3-line imagery which has been taken during the MOMS-02/D2 experiment in spring 1993, and which will be acquired in course of the MOMS-02/PRIRODA project, scheduled for launch in April 1996. The reconstruction of the image orientation is based on a combined adjustment of the complete image, ground control, orbit and attitude information. To this end, the conventional bundle adjustment algorithm is supplemented by a rigorous dynamical modeling of the spacecraft motion to take orbital constraints into account.

The results of the combined adjustment using MOMS-02/D2 imagery and control information of orbit #75B are presented. About 14 000 conjugate points in one imaging sequence covering $430 \times 37\,\text{km}^2$ were processed together with the epoch state vector, attitude data and 12 GPS-derived ground control points (GCP). Within the threefold overlapping area an empirical accuracy of 12 m (0.9 pixel) in planimetry and 7 m (0.5 pixel) in height was achieved as verified by 63 independent check points.

Computer simulations on MOMS-2P image orientation and point determination based on realistic input information have shown that the accuracies of the estimated exterior orientation parameters and object point coordinates will be insufficient, if single strips are processed without any ground control, due to the poor absolute attitude information. Good accuracies, in constrast, can be obtained either with a few precise GCP or even without ground control information, if a block of several overlapping strips with high geometric strength ($q \approx 60\%$) is adjusted.

1 INTRODUCTION

During the 2nd German spacelab mission D2, successfully flown in April/May 1993, the Modular Optoelectronic Multispectral Stereo Scanner MOMS-02 acquired digital high resolution, along track, threefold stereoscopic and multispectral imagery of the earth surface. The MOMS-02/D2 experiment was the first use of a 3-line camera in space. Although the results of this experiment are remarkable, the high accuracy potential of the MOMS-02 sensor couldn't be exhausted due to several problems. These problems, however, have been an important experience in the preparation phase of the forthcoming MOMS-02/PRIRODA (MOMS-2P) mission from the Russian space station MIR, scheduled for April 1996.

The photogrammetric processing of the MOMS-02/D2 and MOMS-2P data is conducted by several German university institutes and the German Aerospace Research Establishment (DLR). The major aim is to realize the entire photogrammetric processing chain, which starts with radiometrically corrected image data and ends up with digital terrain models (DTM), orthoimage maps and vector data for geoinformation systems (GIS). Within the science team the Chair for Photogrammetry and Remote Sensing of the Technical University Munich (TUM) is responsible for the reconstruction of the exterior orientation by combined adjustment and the semi-automatic extraction of linear objects for updating the German GIS ATKIS-DLM25.

After a description of the two camera experiments MOMS-02/D2 and MOMS-2P and the combined block adjustment concept, the results of the adjustment using MOMS-02/D2 imagery of orbit #75B are presented and assessed. Then the results of computer simulations on MOMS-2P image orientation are discussed. Finally the experiences are summarized and an outlook is given.

2 MOMS-02/D2 AND MOMS-2P CAMERA EXPERIMENTS

2.1 MOMS-02/D2 Experiment

The optical system of MOMS-02 consists of a stereo module and a multispectral module (Figure 1). In 7 different imaging modes certain combinations of the panchromatic stereo and the multispectral channels can be selected. The 3 lenses of the stereo module with 1 CCD sensor array (Fairchild 191) each provide 3-fold along track stereo scanning with different ground resolutions. The nadir looking CCD array (4.5 m ground pixel size) comprises 2 arrays with 6000 sensor elements each, which are optically combined to 1 array with 9000 sensor elements. The other CCD arrays of the stereo module consist of 6000 sensor elements (13.5 m ground pixel size). In stereo imaging mode 1 8304 sensor elements of the HR channel and 2976 sensor elements of the stereo channels are active.

In the course of the 10 day lasting D2 mission, 48 data takes with a data volume of 300 GB were recorded during 4.5 h, covering an area of about 7 Mio. km^2. Due to the orbital inclination of 28.5° industrial countries in Europe

	MOMS-02/D2	MOMS-2P
Camera carrier Mission duration Data storage Orbital height [km] Orbital inclination [°] Ground pixel size nadir/stereo [m] Swath width nadir/stereo [km]	Space shuttle 10 days HDT recorder 296 28.5 4.5 / 13.5 37 / 78	MIR space station 18 months onboard mass memory and telemetry to ground stations 400 51.6 6.0 / 18.0 50 / 105
Geometric camera calibration	laboratory	laboratory, inflight
Orbit information	TDRSS tracking	GPS
Attitude information	IMU	IMU, star sensor

Table 1: Main parameters of MOMS-02/D2 and MOMS-2P

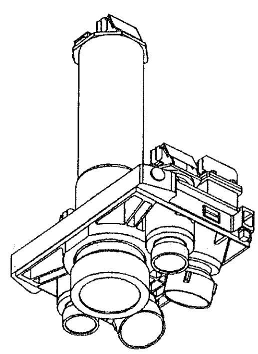

Figure 1: Optical system of the MOMS-02 camera. The two inclined (±21.9°) stereo lenses are depicted in the background. In the foreground, the high resolution lens is visible, arranged between 2 lenses for multispectral data recording.

and North America have not been imaged. More detailed information about the MOMS-02/D2 camera experiment is given by Ackermann et al. (1989), Seige and Meissner (1993) and Fritsch (1995).

To demonstrate the combined adjustment of MOMS-02 imagery using orbital constraints, one imaging sequence with 32 120 rows covering 430×37 km^2 in North-West Australia (orbit #75B) has been chosen (see section 4).

2.2 MOMS-2P Experiment

The MOMS-2P camera is part of the PRIRODA module, which is equipped with several remote sensing instruments. Overall goals of the PRIRODA (russ. *nature*) project are to investigate nature processes and to further develop remote sensing methods (Armand, Tishchenko 1995).

The main parameters of the MOMS-2P experiment are listet in Table 1. In contrast to the D2 mission, the MIR orbital inclination of 51.6° also allows for imaging of industrial countries in Europe and North America. Since MOMS-2P images, acquired during 18 months mission duration, will enable a regional covering, a simultaneous block adjustment of several overlapping strips will be possible.

The camera geometry including the alignment of the MOMS-2P camera axes will be determined not only by calibration in the laboratory, but also by inflight calibration using precise ground control in Catalonia (Iberian Peninsula)(Kornus et al. 1996).

A special navigation package MOMSNAV consisting of high precision GPS and Inertial Measurement Unit (IMU) ensures precise orbit and attitude data, synchronized with the MOMS-2P imagery to 0.1 msec. Based on GPS observations during a time interval of ca. 5 minutes and a sophisticated short arc modelling, the MIR orbit will be determined with 5 m absolute accuracy. The Astro 1 star sensor, which is mounted on the QUANT module of the MIR station provides 10″ attitude accuracy, the alignement, however, between the QUANT and the PRIRODA module will be known only in the order of 200″.

3 COMBINED BLOCK ADJUSTMENT

The photogrammetric point determination is based on the principle of bundle adjustment and comprises the determination of object points and the reconstruction of the exterior orientation of the 3-line images. It represents a central task within the photogrammetric processing chain on which all subsequent products are based.

The collinearity equations

$$\boldsymbol{u} = \boldsymbol{u}(\boldsymbol{x}, \boldsymbol{x}^c(t), \boldsymbol{\theta}(t)) \quad (1)$$

formulate the relationship between the observed image coordinates $\boldsymbol{u} = (u_x, u_y)^T$, the unknown object point coordinates $\boldsymbol{x} = (X, Y, Z)^T$ of a point P and the unknown parameters of exterior orientation $\boldsymbol{x}^c = (X^c, Y^c, Z^c)^T$ and $\boldsymbol{\theta} = (\zeta, \eta, \theta)^T$, respectively, of the image I_j taken at time t. The orientation angles ζ, η and θ have to be chosen in such a way that singularities are avoided. In space photogrammetry the three Euler angles, which are related to the spacecraft motion along the trajectory, are well suited in conjunction with a geocentric object coordinate system.

3.1 Conventional Approach

In general, the mathematical model for the reconstruction of the exterior orientation should use 6 unknown parameters for each 3-line image I_j. In practice, however, there is not enough information to determine such a large number of unknowns. In the conventional approach, the exterior orientation parameters are estimated only for so-called orientation points I_k, which are introduced at certain time intervals, e.g. once for every 1000^{th} readout cycle. In between, the parameters of each 3-line image I_j are expressed as polynomial functions of the parameters at the neighbouring orientation points (Ebner et al. 1994). While this approach reduces the number of unknown exterior orientation parameters to a reasonable amount, its inherent disadvantage is that the estimated position parameters are not associated with a physical model of the spacecraft trajectory.

3.2 Combined Approach

To overcome this drawback, the bundle adjustment algorithm is supplemented by a rigorous dynamical modeling of the spacecraft motion to take orbital constraints into account. The camera position parameters $\boldsymbol{x}^c(t)$ which have been estimated so far at certain time intervals, are now expressed by the 6 parameters of the epoch state vector $\boldsymbol{y}_0$ and additional force model parameters $\boldsymbol{p}$:

$$\boldsymbol{x}^c(t) = \boldsymbol{x}^c(t, \boldsymbol{y}_0, \boldsymbol{p}) \qquad (2)$$

The force model parameters $\boldsymbol{p}$ may comprise e.g. the drag coefficient. Figure 2 demonstrates the combined approach, which exploits the fact that the spacecraft proceeds along an orbit trajectory and all camera positions lie on this trajectory, when estimating the spacecraft's epoch state vector.

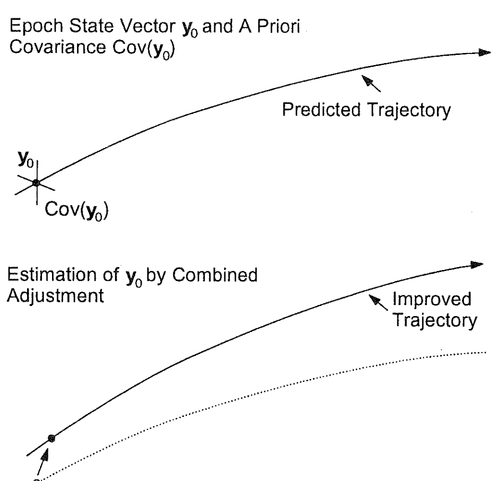

Figure 2: Combined approach for the reconstruction of the exterior orientation of 3-line images (Montenbruck et al. 1994)

Compared to the conventional approach the combined approach has essential advantages, which can be summarized as follows:

- Full utilization of the information content of the tracking data in a statistically consistent way
- A reduced number of unknown parameters
- Accuracy improvements for the photogrammetric results as well as the epoch state vector

Statistically, the resulting estimation procedure is equivalent to a combined orbit determination and bundle adjustment from tracking data and 3-line image data.

Due to the lack of a dynamical model describing the camera's attitude behaviour during an imaging sequence, it is not possible to introduce attitude constraints into the bundle adjustment in a similar way as the orbital constraints. To this end, the concept of orientation points is maintained for the camera's attitude. The attitude

$$\boldsymbol{\theta}(t) = \boldsymbol{\theta}(t, \boldsymbol{\Theta}) \qquad (3)$$

of the camera can be represented by the attitude vector $\boldsymbol{\Theta}$ at selected orientation points. Based on (1), (2) and (3), the image coordinates may finally be written as

$$\boldsymbol{u} = \boldsymbol{u}(\boldsymbol{x}, \boldsymbol{x}^c(t), \boldsymbol{\theta}(t)) = \boldsymbol{u}(t, \boldsymbol{x}, \boldsymbol{y}_0, \boldsymbol{p}, \boldsymbol{\Theta}) . \qquad (4)$$

The mathematical model of the combined approach is described in detail in Montenbruck et al. (1994) and Ohlhof (1996).

4 PRACTICAL RESULTS ON MOMS-02/D2 IMAGE ORIENTATION

4.1 Preprocessing

The first step in the photogrammetric processing chain is the determination of conjugate points in the images. Digital image matching is an appropriate technique to automatically determine these points. Before starting the matching procedure, the image strip of the nadir looking CCD array was resampled by factor 3 to obtain the same pixel size in all 3 strips. Using the least squares *region-growing* matching algorithm (Heipke et al. 1996) about 14 000 conjugate points were found. The standard deviations of the image coordinates were assumed to be 0.3 pixel.

In the area covered by the 3 image strips 79 DGPS-derived natural ground control points (GCP) were available with a standard deviation of 0.1 m in X, Y and Z. 75 points were identified and measured in the images by Baltsavias (1995). Due to difficulties with the localization of the points, the standard deviations of the measured image coordinates were chosen to 0.5 pixel.

During the D2 mission tracking was routinely performed using the Tracking and Data Relay Satellite System (TDRSS). The orbit determination for orbit #75B is based on 900 S-Band Doppler measurements with a sampling rate of 10 s covering about 180 minutes. The force modeling comprises the drag coefficient and 5 parameters describing perturbations caused by the attitude thruster system. The pure statistical standard deviations of the epoch state vector components were 30 m in X, Y, Z, whereas unmodeled effects resulting from the attitude thruster system contribute an additional error of up to 50 m in X, Y and Z (Braun, Reigber 1994).

A major problem arose from the fact that the image recording times could only approximately be related to the time scale UTC of the orbit and attitude information. Since no parameter for the time offset exists in the bundle adjustment algorithm, a realistic weighting matrix for the epoch state vector components has been derived relaxing the orbital constraints in the along-track direction (Gill et al. 1995).

Attitude information was derived from gyro recordings of the IMU of the shuttle Guidance Navigation and Control System. Based on approximation tests the optimum distance between two orientation points was found to be 4615 rows, corresponding to a flight distance of 62.3 km and a flight time of 9.1 s.

4.2 Combined Adjustment

The combined adjustment was performed in the geocentric coordinate system WGS84. The DGPS-derived GCP were divided into two groups. The first group consists of 12 GCP, where 3 points each are located in the corners of the threefold overlapping area to ensure a precise definition of the global datum. The second group comprises 63 geometrically well distributed points which were used as check points.

The following data were introduced as observations:

- Image coordinates of 13 959 conjugate points ($\sigma = 0.3$ pixel)
- Image coordinates of 12 GCP ($\sigma = 0.5$ pixel)
- Image coordinates of 63 check points ($\sigma = 0.5$ pixel)
- Object coordinates of 12 GCP ($\sigma_X = \sigma_Y = \sigma_Z = 0.1$ m)
- Epoch state vector components with associated 6×6 weighting matrix
- Attitude parameters (ζ, η, θ) at 8 orientation points ($\sigma_\zeta = \sigma_\eta = \sigma_\theta = 50''$)

In Table 2 the rms values of the theoretical standard deviations of the check point coordinates $\hat{X}$, $\hat{Y}$ and $\hat{Z}$ and the corresponding empirical values are presented. The theoretical values were computed from the inverted normal equation matrix and the a posteriori $\hat{\sigma}_0$ value of the combined adjustment. The empirical values were derived by comparing the estimated object coordinates of the check points and the known values.

MOMS #75B		theor.	empir.
$\mu_{\hat{X}}$	[m]	11.2	9.3
$\mu_{\hat{Y}}$	[m]	13.1	10.2
$\mu_{\hat{Z}}$	[m]	8.9	11.2
$\mu_{\hat{X}\hat{Y}\hat{Z}}$	[m]	11.2	10.3

Table 2: Rms values $\mu_{\hat{X}}$, $\mu_{\hat{Y}}$, $\mu_{\hat{Z}}$ and $\mu_{\hat{X}\hat{Y}\hat{Z}}$ of the theoretical standard deviations derived from 63 check points and corresponding empirical values

The good correspondence between the theoretical and the empirical values indicates the correctness of the stochastic and the functional model. The empirical values show that accuracies of about 10 m (0.7 pixel) in X, Y and Z were achieved. Note that these accuracies are related to the global WGS84 coordinate system. The empirical accuracy referring to a local topocentric coordinate system amounts to 11.8 m in planimetry and 7.3 m in height. The planimetric accuracy is impaired by localization problems of the GCP and check points in the images. A graphical analysis of the residuals in the check points showed that the results are not affected by systematic errors.

5 COMPUTER SIMULATIONS ON MOMS-2P IMAGE ORIENTATION

A series of computer simulations have been carried out to analyze the effect of certain parameters on the accuracy of MOMS-2P image orientation, especially the effect of block configuration and control information.

5.1 Input Parameters

a) Block Configurations

The computer simulations were performed for 3 different block configurations:

- Single strip
- Block of 6 strips with $q = 20\%$ side overlap
- Block of 11 strips with $q = 60\%$ (Figure 3)

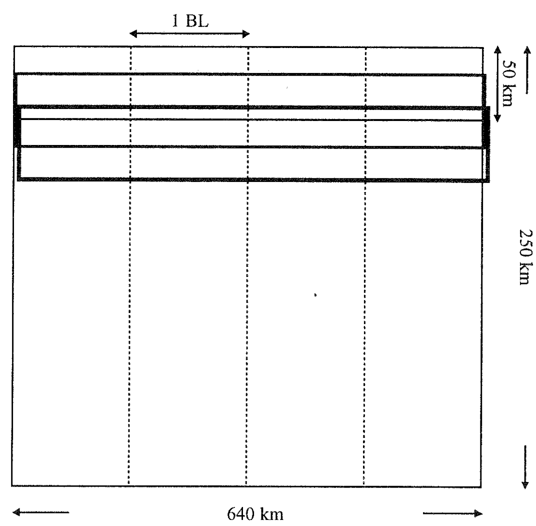

Figure 3: Block consisting of 11 strips with 4 baselengths each and 60% side overlap

The strip length was chosen to 4 baselengths (640 km). This results in the fact that points at the beginning and the end of the single strip are projected into 2 images only, whereas each point in the central part of the strip is projected into 3 images. The strip width amounts to 50 km. The entire block covers 320×250 km^2 (without 2-ray area), corresponding to the area of Catalonia (270×250 km^2), which is the most important calibration site of the MOMS-2P experiment.

b) Interior Orientation Parameters

All parameters of the interior orientation were introduced as error-free values.

c) Conjugate Points

The object coordinate system is defined as topocentric Cartesian system XYZ with the positive direction of the

X-axis parallel to the direction of flight. The object points are arranged in a grid with $\Delta X = 12.5$ km, $\Delta Y = 12.5$ km and $Z = 0$ km. Consequently the single strip consists of 260 and the blocks contain 1,092 object points. For each block configuration, the image coordinates of the object points were computed assuming a straight forward flight path with a constant altitude of 400 km and attitude values equal to zero. All image coordinates were treated as being uncorrelated with equal standard deviations of 0.3 pixel.

d) Ground Control Information

Either no or 16 GCP with $\sigma_X = \sigma_Y = \sigma_Z = 1.0$ m were used. The 16 GCP are arranged in 4 groups of 4 points each, located at the corners of the 3-ray area of the strip or the block. The standard deviations of the image coordinates are assumed to 0.5 pixel.

e) Orbit and Attitude Observations

For the orbit and attitude observations 3 different cases were investigated (Tables 3 and 4). Case B is the most realistic one. In Table 3 the standard deviations describing the relative accuracy of the position parameters are zero, since all camera positions are constrained to lie on the orbit trajectory. The standard deviations describing the absolute accuracy are 5 m for the position and 2 cm/s for the velocity components of the epoch state vector.

		Position		
		A	B	C
relative		0 m	0 m	0 m
absolute	position	0 m	5 m	20 m
	velocity	0 cm/s	2 cm/s	8 cm/s

Table 3: Standard deviations of the observed position parameters

		Attitude		
		A	B	C
relative		0″	10″	20″
absolute	bias	0″	200″	no obs.
	drift	0″/s	0.7″/s	no obs.

Table 4: Standard deviations of the observed attitude parameters

For each orientation point attitude observations were introduced with a relative accuracy of 10″ and an absolute accuracy of 200″ (bias) and 0.7″/s (drift) respectively (Table 4). Besides case B, two extreme cases are investigated for comparison: error-free (A) and worst case (C) orbit and attitude observations. Based on experiences with MOMS-02/D2 data, the distance between the orientation points was chosen to 4,940 rows (ca. 90 km) leading to 9 orientation points per strip.

5.2 Results

For analysis, the rms values $\mu_{\hat{X}\hat{Y}}$ (planimetry) and $\mu_{\hat{Z}}$ (height) of the theoretical standard deviations $\sigma_{\hat{X}}$, $\sigma_{\hat{Y}}$ and $\sigma_{\hat{Z}}$ of all 3-ray points (single strip), 3- and 6-ray points (block with $q = 20\%$) as well as 3-, 6- and 9-ray points (block with $q = 60\%$) were calculated. Moreover, the rms values $\mu_{\hat{\omega}}$, $\mu_{\hat{\varphi}}$, $\mu_{\hat{\kappa}}$ of the theoretical standard deviations of the estimated exterior orientation parameters $\hat{\omega}$, $\hat{\varphi}$, $\hat{\kappa}$ at the orientation points were computed. All accuracy figures were derived from the inverted normal equation matrix.

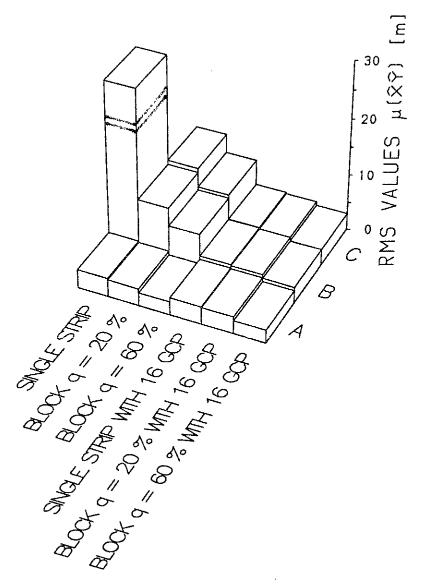

Figure 4: Rms values $\mu_{\hat{X}\hat{Y}}$ for different block configurations, ground control information and orbit/attitude data

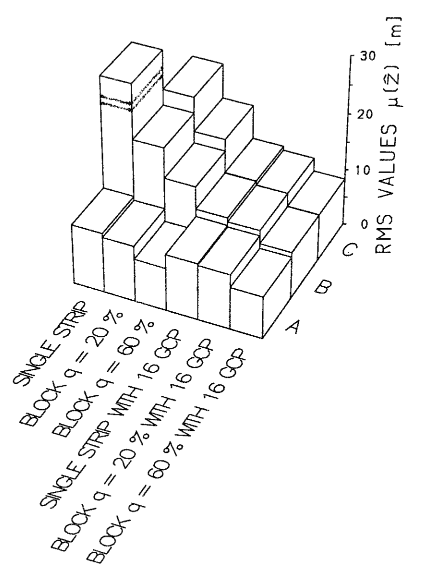

Figure 5: Rms values $\mu_{\hat{Z}}$ for different block configurations, ground control information and orbit/attitude data

In Figures 4–8 these rms values are shown graphically, where A,B and C stand for the standard deviations of the observed position and attitude parameters according to Tables 3 and 4.

First the results of the single strip adjustments without GCP are discussed. Assuming error-free position and attitude data (A), the accuracy of point determination only depends on the standard deviations of the image coordinates, the number of conjugate points and the geometric constellation of the ray intersections. The rms values are 3 m in planimetry and 10 m in height.

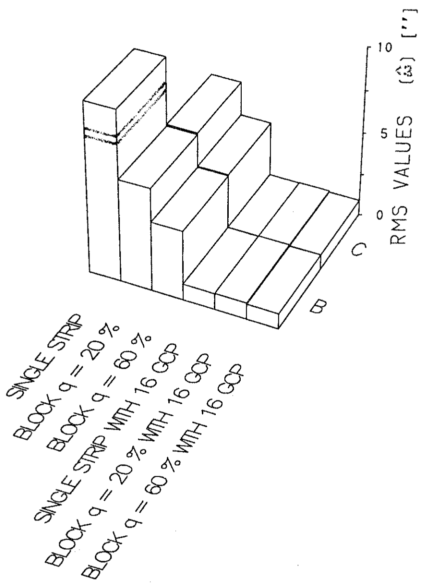

Figure 6: Rms values $\mu_{\hat{\omega}}$ for different block configurations, ground control information and orbit/attitude data

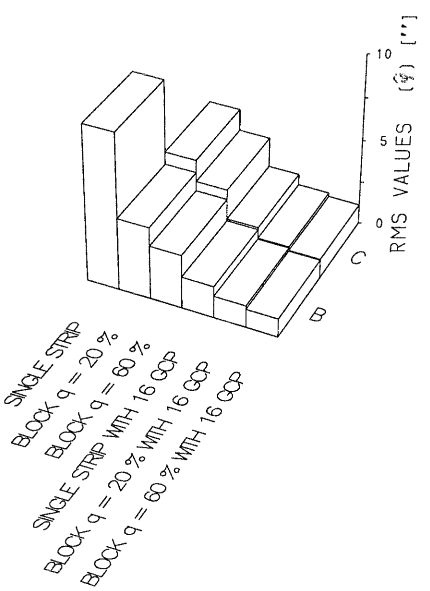

Figure 7: Rms values $\mu_{\hat{\varphi}}$ for different block configurations, ground control information and orbit/attitude data

The planimetric and height accuracies decrease, if the position and attitude data are introduced with realistic standard deviations (case B). The rms values amount to $\mu_{\hat{X}\hat{Y}}$ = 277 m and $\mu_{\hat{Z}}$ = 50 m. They are too high to be shown true to scale in Figures 4 and 5. The reason for these unfavourable values is the poor absolute accuracy of 200″ (bias) and 0.7″/s (drift) of the observed attitude parameters ω. For the single strip this accuracy cannot be improved by the adjustment. Consequently, the rms value $\mu_{\hat{\omega}}$ amounts to 201″. Figure 6 is not able to show this high value true to scale.

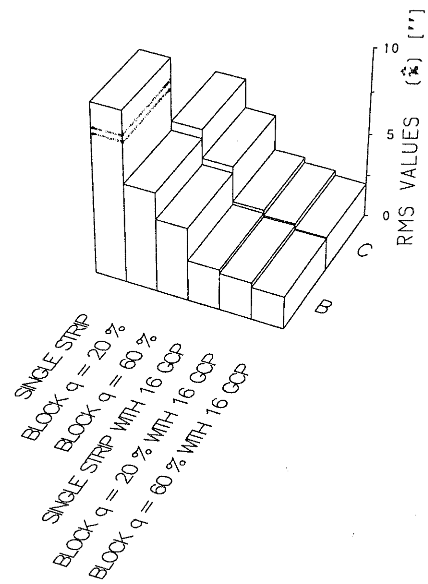

Figure 8: Rms values $\mu_{\hat{\kappa}}$ for different block configurations, ground control information and orbit/attitude data

Case C leads to a singular configuration because for bias and drift of ω no observations are available, and any other observations are not able to determine the unknowns $\hat{\omega}$.

Next the results of the block adjustments without GCP are analyzed. The accuracies which are achieved for the single strip (case B) can be improved considerably, if a block with $q = 20\%$ is adjusted ($\mu_{\hat{X}\hat{Y}} = 11$ m, $\mu_{\hat{Z}} = 20$ m). The roll angles $\hat{\omega}$ are now determined with an accuracy of $\mu_{\hat{\omega}} = 6''$ due to the absolute position data, which were introduced for each strip of the block. The accuracies are only slightly poorer for case C.

In case of the block with $q = 60\%$ the accuracies of both, object coordinates and orientation parameters are improved by a factor of about 1.4 compared with the $q = 20\%$ block. For the object coordinates $\mu_{\hat{X}\hat{Y}} = 8$ m and $\mu_{\hat{Z}}$ = 15 m (case B) can be obtained, that is by factors 3.2 (planimetry) and 2 (height) poorer than in case A.

In the following the adjustment results using GCP are discussed. Figures 4–8 show that high accuracies are obtained if 16 GCP are incorporated into the bundle adjustment. In Figures 4 and 5 the rms values of cases B and C are close to the ones of case A with error-free orbit and attitude data, even in case of single strips ($\mu_{\hat{X}\hat{Y}} = 4$ m and $\mu_{\hat{Z}} = 11$ m for B). Using the equal number of GCP the accuracies improve slightly for the $q = 20\%$ blocks and considerably for the $q = 60\%$ blocks due to the increasing block strength. The blocks with $q = 60\%$ provide rms values of $\mu_{\hat{X}\hat{Y}} = 3$ m, $\mu_{\hat{Z}} = 8$ m and $\mu_{\hat{\omega}} = 1''$, $\mu_{\hat{\varphi}} = 1''$, $\mu_{\hat{\kappa}} = 2''$ respectively, for B and C.

Finally, it can be stated that all exterior orientation parameters are estimated with high accuracy, if a few precise GCP are combined with position data of high relative accuracies.

The observations of the star sensor providing absolute attitude information are necessary for single strip adjustment *without* GCP, but dispensable for single strips *with* GCP and for blocks.

6 SUMMARY AND OUTLOOK

The reconstruction of the image orientation of the MOMS-02 camera is based on a combined adjustment of the complete image, ground control, orbit and attitude information. To this end, the conventional bundle adjustment algorithm is supplemented by a rigorous dynamical modeling of the spacecraft motion to take orbital constraints into account.

The results of the combined adjustment using MOMS-02/D2 imagery and control information of orbit #75B are presented. About 14 000 conjugate points in one imaging sequence covering 430×37 km^2 were processed together with the epoch state vector, IMU data and 12 GPS-derived GCP. Within the threefold overlapping area an empirical accuracy of 12 m (0.9 pixel) in planimetry and 7 m (0.5 pixel) in height was achieved as verified by 63 independent check points.

Computer simulations on MOMS-2P image orientation and point determination based on realistic input information have shown that the accuracies of the estimated exterior orientation parameters and object point coordinates will be insufficient, if single strips are processed without any ground control, due to the poor absolute attitude information. Good accuracies, in constrast, can be obtained either with a few precise GCP or even without ground control information, if a block of several overlapping strips with high geometric strength ($q \approx 60\%$) is adjusted.

Further computer simulations on MOMS-2P image orientation will be performed to analyze the influence of the number of conjugate points and of the accuracy of the interior orientation parameters on the final results. Moreover, the role of the orbit and attitude observations with their relative and absolute accuracies will be investigated in more detail.

7 ACKNOWLEDGEMENT

The work presented in this paper is funded by grants 50 QS 9008 and 50 QM 9205 of the German Space Agency (DARA).

8 REFERENCES

Ackermann F., Bodechtel J., Lanzl F., Meissner D., Seige P., Winkenbach H. (1989): MOMS-02 — Ein multispektrales Stereo-Bildaufnahmesystem für die zweite deutsche Spacelab-Mission D2; Geo-Information-Systems **2**(3), 5–11.

Armand N.A., Tishchenko Y.G. (1995): Russian PRIRODA Project Space Experiments With MOMS-2P; Presented paper at the MOMS symposium, July 5–7, Cologne.

Baltsavias E. (1995): Personal communication.

Braun C.v., Reigber C. (1994): Space shuttle orbit determination using empirical force modelling of attitude maneuvers for the German MOMS-02/D2 mission; Flight Mechanics and Estimation Theory Symposium, Goddard Space Flight Center, May 17-19, Greenbelt.

Ebner H., Kornus W., Ohlhof T. (1994): A simulation study on point determination for the MOMS-02/D2 Space Project using an extended functional model; Geo-Information-Systems **7**(1), 11–16.

Fritsch D. (1995): Ableitung digitaler Geländemodelle aus MOMS02/D2-Bilddaten — erste Ergebnisse; Geo-Information-Systems **8**(2), 13–20.

Gill E., Montenbruck O., Ohlhof T., Schmidhuber M. (1995): First results on shuttle orbit adjustment using MOMS-02 imagery; Proceedings of the International Space Dynamics Symposium, June 19-23, Toulouse, 917–929.

Heipke C., Kornus W., Pfannenstein A. (1996): The Evaluation of MEOSS Airborne Three-Line Scanner Imagery: Processing Chain and Results; Photogrammetric Engineering & Remote Sensing **62**(3), 293–299.

Kornus W., Lehner M., Blechinger F., Putz E. (1996): Geometric Calibration of the Stereoscopic CCD-Linescanner MOMS-2P; Presented paper at the XVIII. ISPRS Congress, July 9–19, Commission I, Vienna.

Montenbruck O., Gill E., Ohlhof T. (1994): A Combined Approach for Mars-94 Orbit Determination and Photogrammetric Bundle Adjustment; DLR-Forschungsbericht 94-13, 95 p.

Ohlhof T. (1996): Lokale, regionale und globale Punktbestimmung mit Dreizeilenbilddaten und Bahninformation der Mars96-Mission. Deutsche Geodätische Kommission, C 445, 139 p.

Seige P., Meissner D. (1993): MOMS-02: An advanced high resolution multispectral stereo scanner for Earth observation; Geo-Information-Systems **6**(1), 4–11.